Simultaneous adsorption/reduction of bromate in water using nano zero-valent iron supported on ordered mesoporous silica

Xiaodong Xin, Shaohua Sun, Mingquan Wang, Qinghua Zhao, Wei Li and Ruibao Jia

ABSTRACT

Bromate is mainly produced by ozone oxidation, and it is a kind of highly toxic substance in drinking water and a serious threat to people's health. It is difficult to remove it using traditional processes. The reduction of nano zero-valent iron (nZVI) has proved to be an effective method to remove bromate in water. In this study, we designed and prepared a new kind of nanocomposite by loading nZVI into ordered mesoporous silica materials (nZVI/MCM-41), which avoided nZVI oxide and increased adsorption at the same time. The removal efficiencies of bromate by MCM-41, nZVI, and nZVI/MCM-41 were evaluated respectively. The result indicated that nZVI/MCM-41 showed the highest removal efficiency for bromate at pH 6.5, with an appropriate dose of 25 mg when initial bromate concentration was 0.2 mg/L. In the removal process, adsorption and reduction exist at the same time and reduction was the leading role. Kinetic studies showed that the removal of bromate by nZVI/MCM-41 followed pseudo-first-order kinetics. Finally, bromine mass balance demonstrated that bromide was the only product for bromate reduction, suggesting that bromate was first adsorbed onto nZVI/MCM-41 and reduced to innocuous bromide by nZVI subsequently.

Key words | bromate, loaded type nano zero-valent iron, product analysis, removal mechanism

Xiaodong Xin
Shaohua Sun
Mingquan Wang
Qinghua Zhao
Wei Li
Ruibao Jia (corresponding author)
Shandong Province City Water Supply and
    Drainage Water Quality Monitoring Center,
Jinan 250101,
China
E-mail: jiaruibao1968@163.com

INTRODUCTION

Nowadays, with the improvement of people's living standards, more attention has been paid to the safety of drinking water. Drinking water disinfection was one of the most effective measures for the maintenance of public health in the 20th century, and it is also an effective means for the prevention of epidemics spreading through water. But water disinfectants can react with materials in the water such as organic matter, bromine and iodine, which could produce a series of disinfection by-products threatening to human health (Hwang & Jaakkola 2003; Nieuwenhuijsen 2005; Hrudey 2009). There are about 600 kinds of disinfection by-products that have been reported at present (Richardson 2005; Krasner et al. 2006). Bromate (BrO_3^-) is mainly produced by ozone oxidation, and is a highly toxic substance that could cause

cancer for animals (Gunten 2003; Weinberg et al. 2003). Bromate has been classified as a group 2B or possible human carcinogen by the International Agency for Research on Cancer (Moore & Chen 2006). The maximum contaminant level for bromate in drinking water established by the World Health Organization is only 10 μg/L (Weinberg et al. 2003). However, it has been found that bromate concentration is 150 μg/L following ozonation of drinking water (Krasner et al. 1993). Thus, the removal of bromate in water has become a matter of interest.

At present, different approaches have been taken to remove bromate in water, including adsorption, reduction, advanced oxidation, biological degradation, and so on (Ginkel et al. 2005; Meunier et al. 2006; Wiśniewski &

Kabsch-Korbutowicz 2010; Chitrakar *et al.* 2011). Due to the hydrophilia and oxidability of bromate, the chemical reduction process has proved to be an efficient and cost-effective method. Nano zero-valent iron (nZVI) is widely applied in various organic and inorganic contaminant reduction due to its good reducibility and large specific surface area (Cho *et al.* 2015; Ling *et al.* 2015; Liu *et al.* 2015; Nakatsuji *et al.* 2015; Segura *et al.* 2015). There has been little research on bromate removal by zero-valent iron with higher concentration of bromate (Xie & Shang 2007; Lin & Lin 2017).

Like many other nanomaterials, nZVI particles easily agglomerate into large particles, resulting in a decrease of surface area and reactivity performance, which has limited its application in water treatment (Phenrat *et al.* 2006). Therefore, researchers have paid attention to the modification of nano zero-valent iron (Chun *et al.* 2010; Wang *et al.* 2010; Jia *et al.* 2011; Zhang *et al.* 2011; Xu *et al.* 2014). Immobilization of nZVI in a mesoporous material is a promising approach to solve the problem above (Li *et al.* 2011; Lv *et al.* 2011; Zhou *et al.* 2016). Mesoporous materials with large specific surface area, uniform aperture adjusted, morphology and active surface groups came onto people's horizons. They are widely used in macromolecule adsorption and separation, biological medicine, chemical catalysis, chemical sensors, and the synthesis of nanomaterials (Wakayama *et al.* 2003; Chytil *et al.* 2005; Fan *et al.* 2005; Kong *et al.* 2010). Mesoporous silica has attracted intense interest due to its adsorption capacity, high surface area, porous structure, and relatively low cost. Mesoporous silica MCM-41 has been proven to be generally quite effective for iron loading (Pan *et al.* 2013; Liu *et al.* 2014). The combination of MCM-41 and nZVI would take advantage of the two materials. It is interesting to evaluate the efficiency of bromate adsorption/reduction by nZVI supported on MCM-41.

In this study, we designed and prepared a new kind of nanocomposite by loading nano zero-valent iron into ordered mesoporous silica materials (nZVI/MCM-41), which avoided zero-valent iron oxide and increased adsorption at the same time. The materials were used to remove bromate in water. The characterization of the synthesized nZVI/MCM-41 was performed, and the applicability of nZVI/MCM-41 in bromate removal was evaluated with

regard to the operating variables on the reduction–adsorption process. The prepared nZVI/MCM-41 showed excellent reductive performance for bromate.

EXPERIMENT

Materials and chemicals

All chemicals, obtained from Sinopharm Chemical Reagent Beijing Co. Ltd, China, are of analytical reagent grade or better quality. Ultrapure water was used throughout the experiment (18.2 MΩcm).

Synthesis of nZVI/MCM-41

MCM-41 was synthesized as by Dimos *et al.* (2009). An amount of 50 g tetraethylorthosilicate was added in a polyethylene bottle containing 417.5 g H_2O, 268.5 g NH_3 (25% wt) and 10.5 g cetyltrimethylammonium bromide, and stirred for 30 min. After heat treatment at 80 °C for 96 h, the product was retrieved. It was filtered, rinsed with cold ethanol and finally placed on a plate for air-drying.

The nZVI/MCM-41 was prepared by the liquid phase reduction method as according to Petala *et al.* (2013). Typically, $FeSO_4 \cdot 7H_2O$ (8.93 g) was dissolved in ethanol/water (4/6) solution (100 mL), followed by the addition of polyethylene glycol-4000 (0.125 g/g). MCM-41 (20 g) was added into the above solution and stirred well. Then, $NaBH_4$ solution (0.45 mol/L) was added into the above mixed solution drop by drop. All of the reactions were conducted under an anaerobic environment. After reaction, the products were washed three times with ethanol, acetone, and anaerobic water respectively. The resulted precipitates (nZVI/MCM-41) were ready for use.

Characterization

The morphological structure and dispersion of nZVI/MCM-41 were observed by scanning electron microscopy (SEM) (ZEISS, Germany). All SEM specimens were sputter-coated with a thin layer of gold palladium under vacuum in an argon atmosphere prior to examination. X-ray diffraction (XRD) patterns of the prepared samples were acquired with a Rigaku

D/MAX 2200 X-ray diffractometer (Tokyo, Japan) using CuKα radiation (40 kV, 300 mA) of wavelength 0.154 nm to confirm the structure of the materials. Surface area measurements were performed on a Micromeritics ASAP 2020 surface area and porosity analyzer (Quantachrome, USA). Bromate was detected by an ion chromatograph (ICS-3000, USA). Fe was detected by inductively coupled plasma mass spectrometry (ICP-MS) (NexIon 300x, Perkin Elmer, USA).

Batch experiment for BrO_3^- adsorption/reduction

In a typical batch experiment, 25 mg of the as-prepared nZVI/MCM-41 was added into 500 mL of mixed solution containing 0.2 mg/L of bromate, the mixture was adjusted to pH 6 with HCl and NaOH and stirred for 60 min, and then nZVI/MCM-41 were separated from filter separation. In order to obtain the removal isotherms, bromate solutions with varying initial concentration of individual bromate were treated with the same procedure as above at room temperature.

The removal efficiency and the amount of bromate removed q (mg/g) were given according to the formula:

$$\text{Removal efficiency}\,(\%) = \frac{c_0 - c_t}{c_0} \times 100\% \tag{1}$$

$$q_t = \frac{(c_0 - c_t) \times V}{m} \tag{2}$$

where c_t (mg/L) is the concentration of bromate at time t (min), V (L) is the volume of the bromate solution, m (g) is the mass of nZVI/MCM-41; q_e (mg/g) is the removal amount at equilibrium, q_t (mg/g) is the adsorbed amount at time t (min).

RESULTS AND DISCUSSION

Characterization of nZVI/MCM-41

The surface morphology of nZVI/MCM-41 can be seen from Figure 1(b). Compared with Figure 1(a), after loading nano zero-valent iron, a layer of spherical particles adheres on the surface of the MCM-41 and is evenly distributed.

The XRD patterns of MCM-41 and nZVI/MCM-41 are presented in Figure 1(c). Figure 1(c) compares the X-ray diffraction pattern of before and after nZVI is loaded in the MCM-41. There is an obvious zero-valent iron characteristic peak at $2\theta = 43°–45°$ (α-Fe^0), which is accordance with the report of Cho *et al.* (2015). It indicated that nZVI has been successfully loaded on the MCM-41.

According to the Brunauer-Emmett-Teller (BET) analysis, after loading nZVI, the Barrett-Joyner-Halenda (BJH) desorption cumulative volume of pores of nZVI/MCM-41 is 0.1776 cm^3/g, which is smaller than MCM-41 (0.5973 cm^3/g), and the BET surface area is 303 m^2/g, which is smaller than MCM-41 (745 m^2/g).

Effect of operating variables on the removal of bromate onto nZVI/MCM-41

Comparison of different materials on removal

Three kinds of materials, nZVI, MCM-41, and nZVI/MCM-41 were used to remove 500 mL 0.2 mg/L bromate. From
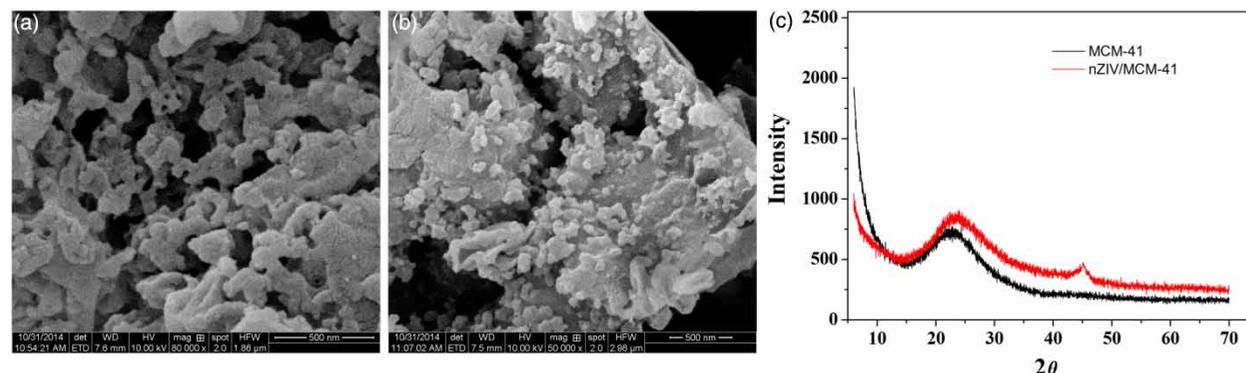

Figure 1 | Scanning electron microscopy of (a) MCM-41, (b) nZIV/MCM-41 and XRD diffraction patterns of (c) MCM-41 and nZIV/MCM-41.

Figure 2(a), it is clear that the removal capacity of nZVI/MCM-41 is better than that of nZVI and MCM-41. Therefore, nZVI/MCM-41 was used to remove the bromate.

Effect of nZVI/MCM-41 concentration

To determine the effect of nZVI/MCM-41 dose, the 2 h uptake experiments were carried out at 25°C with the nZVI/MCM-41 dosage ranging from 10 to 45 mg in 500 mL 0.2 mg/L bromate solution. As shown in Figure 2(b), the removal of bromate increased with the increase of nZVI/MCM-41 dose, and reached a plateau at the appropriate dose of 25 mg; 25 mg of nZVI/MCM-41 was chosen for the test.

Effect of initial pH

The pH value of the solution was an important controlling parameter in the removal process. The removal of bromate onto nZVI/MCM-41, nZVI and MCM-41 increased significantly with increasing pH from 4 to 6.5, and decreased from 6.5 to 9 (Figure 2(c)). At different pH, the removal efficiency of nZVI/MCM-41 was larger than that of nZVI and

MCM-41. It can be illustrated that too much acidity or alkalinity could reduce the bromate removal rate of nZVI/MCM-41. Under pH 6.5, the removal effect of bromate on nZVI/MCM-41 was better.

The reaction time

An amount of 25 mg nZVI/MCM-41 was added into 0.2 mg/L of bromate solution and the remaining amounts of bromate at 1, 5, 10, 20, 30, 40, 60, 90, 120, 150, 180, 240 min respectively were detected. In Figure 2(d), the removal efficiency of nZVI was low in the first 90 min (lag period), increased after 90 min and got to equilibrium after 240 min (reaction period), which also showed that the removal rate of nZVI/MCM-41 was faster than that of nZVI. Reaction kinetics needed to be used to confirm it.

The concentrations of Fe in solution with different reaction times were also detected, which is shown in Figure 2(e). With the increased reaction time, the concentration of Fe increased and reached equilibration after 90 min, which was in accord with the removal time by nZVI/MCM-41. It can be concluded that the bromate removal by nZVI/MCM-41 was related to nZVI.
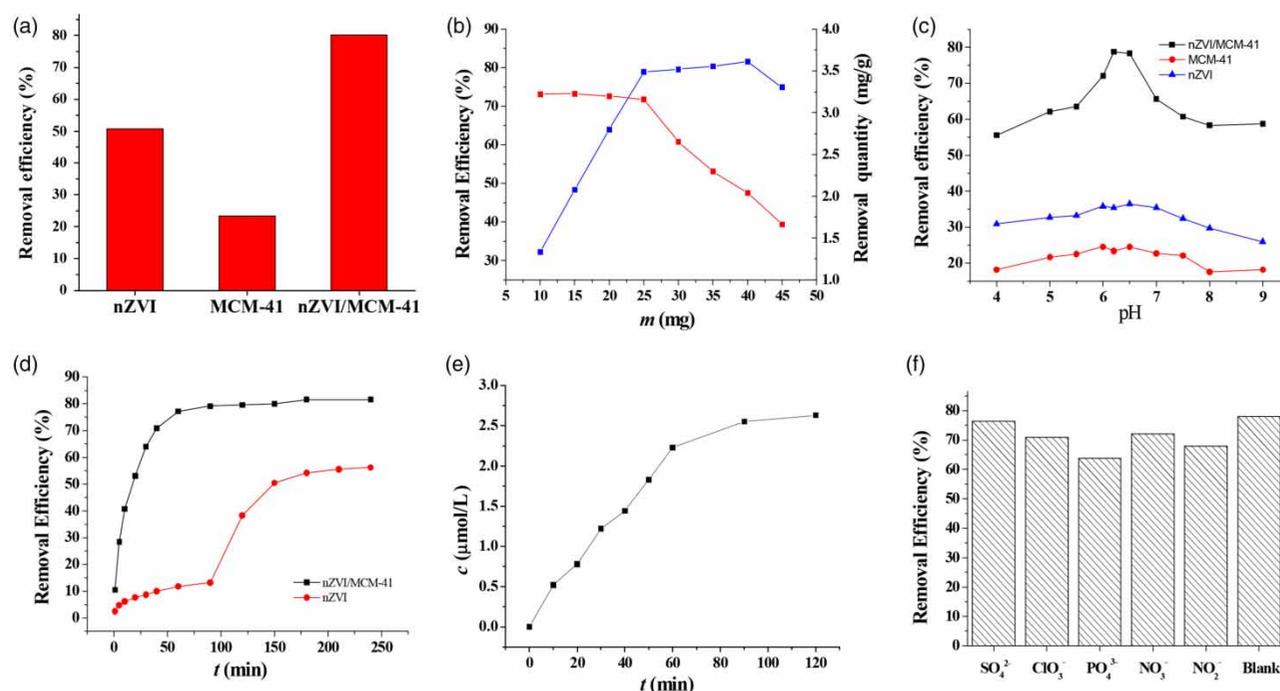

Figure 2 │ (a) Effect of materials, (b) nZVI/MCM-41 dose, (c) initial pH, (d) performing time, (e) Fe concentration with reaction time, (f) and inorganic anions.

Effect of inorganic anions

When other inorganic ions exist in solution, it may affect bromate removal. Several kinds of common anions in water were chosen, such as PO_4^{3-}, NO_3^-, NO_2^-, SO_4^{2-}, ClO_3^-. The sample was pure water with only 0.2 mg/L bromate. The concentrations of PO_4^{3-}, NO_3^-, NO_2^-, SO_4^{2-}, ClO_3^- added into the sample were 1 mg/L, 10 mg/L, 1 mg/L, 200 mg/L, and 1 mg/L, respectively. From Figure 2(f), it can be found that these ions have different effects on the removal of the bromate. The effect of PO_4^{3-} was larger than that of the others, reducing bromate removal efficiency by 24%, the others by no more than 15%. The reason may be that these ions could react with zero-valent iron, competing with bromate, which reduced bromate removal efficiency. We also detected the concentrations of five common anions before and after the removal. The concentrations of the five common anions after the removal decreased about 15–22%, except PO_4^{3-}, which decreased about 32%. Previous studies (Khalil *et al.* 2017; Sleiman *et al.* 2017) indicated that zero-valent iron could remove PO_4^{3-}, which was in accordance with our result. That proves our reasoning: these ions could react with zero-valent iron, competing with bromate.

Reaction kinetics

In order to investigate the mechanism of reduction and potential rate-limiting steps such as mass transport and chemical reduction reaction processes, the reaction time data of bromate onto nZVI/MCM-41 and nZVI were analyzed with kinetic models, such as the pseudo-first-order kinetic model and pseudo-second-order kinetic model.

Pseudo-first-order model:

$$\frac{dq_t}{dt} = k_{obs}\,(q_e - q_t) \tag{3}$$

Pseudo-second-order model:

$$\frac{dq_t}{dt} = k_2\,(q_e - q_t)^2 \tag{4}$$

Figure 3 shows that the measured kinetic data of bromate adsorbed by nZVI/MCM-41 fitted the pseudo-first-order kinetic model with a correlation coefficient (R^2) of 0.997 and 0.998. The rate constant (k_{obs}) of nZVI/MCM-41 and nZVI was 0.0712 min^{-1} and 0.0169 min^{-1}, respectively. The results showed that the reduction process of nZVI/MCM-41 is much faster than that of nZVI.

Reaction thermodynamics

The influence of temperature on bromate removal onto nZVI/MCM-41 was carried out at temperatures ranging from 293 to 313 K. Under different temperatures, the adsorption capacities of the as-obtained nZVI/MCM-41 for bromate were measured individually at pH 6.5 with 25 mg of nZVI/MCM-41 and bromate concentration 0.1–0.8 mg/L.

The thermodynamic equilibrium constants (K_d) of the adsorption–reduction process, i.e. the constants for bromate distribution between the solid and liquid phases at equilibrium, were computed using the method of Lyubchik (Lyubchik *et al.* 2004) by plotting $\ln(q_e/c_e)$ versus q_e and extrapolating q_e to zero under different temperatures, which is shown in Figure 4 with the correlation coefficient of 0.99. The thermodynamic parameters are listed in Table 1. The negative values of Gibbs free energies (ΔG) and positive values of ΔH indicate that the removal of bromate onto nZVI/MCM-41 is spontaneous and endothermic.

$$\Delta G = -RT \ln K_d \tag{5}$$

$$\ln K_d = \frac{\Delta S}{R} - \frac{\Delta H}{RT} \tag{6}$$

Mechanism of bromate removal by nZVI/MCM-41

In order to reveal the removal process, it is necessary to analyze the product. After adsorption/reduction of nZVI/MCM-41, bromide ions can be detected. Figure 5 illustrates that bromide was the only product for bromate reduction, and the bromate balance was in the range of 83–102% during the experimental course, indicating that the removal of bromate by nZVI/MCM-41 was dominantly due to the reduction of nZVI instead of adsorption by nZVI/MCM-41.

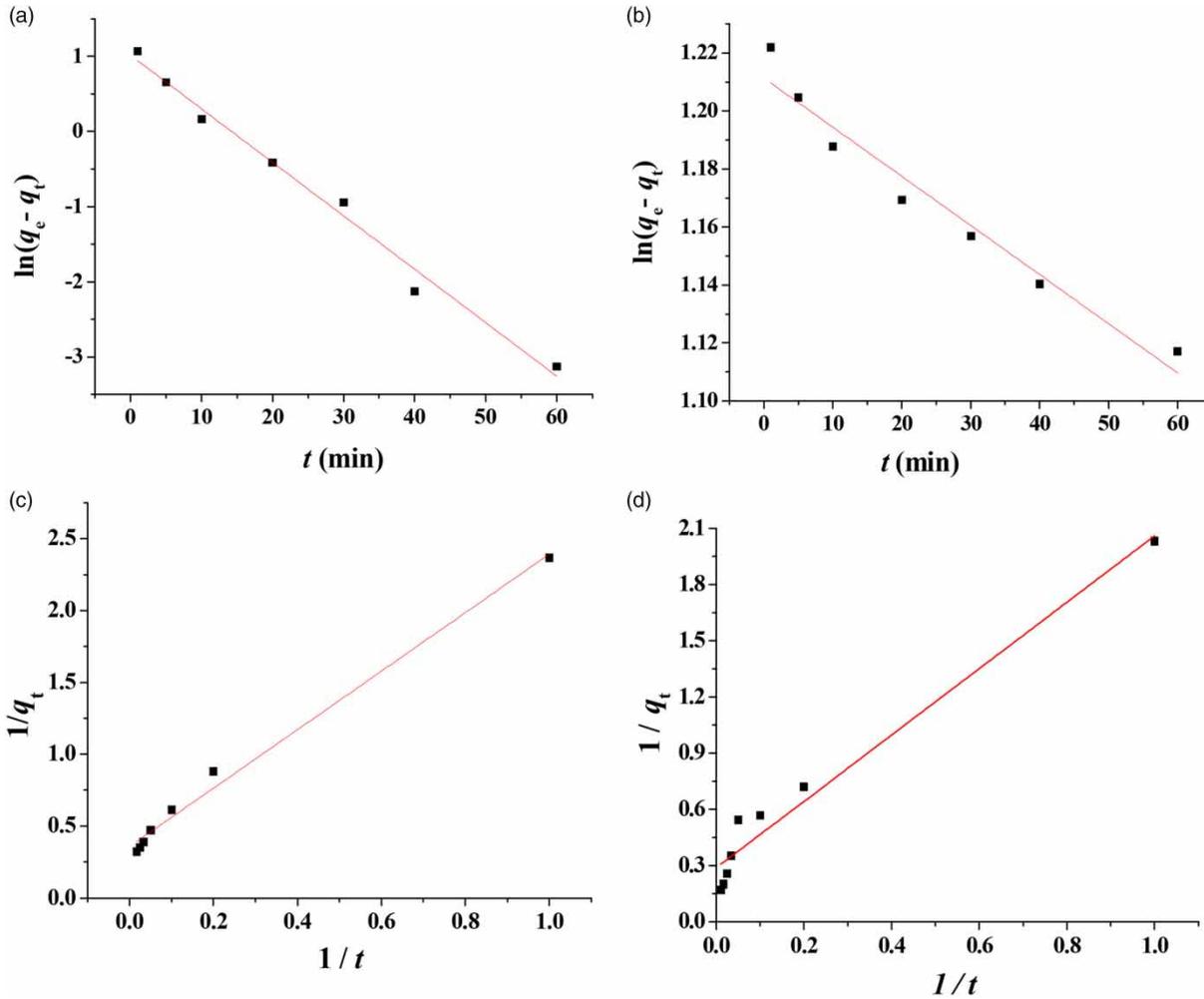At the first 5 minutes, few bromine ions were found in the solution and bromate concentration in the solution

Figure 3 | (a, b) First-order kinetics and (c, d) second-order kinetics fit of bromate adsorption on nZIV/MCM-41 and nZIV.
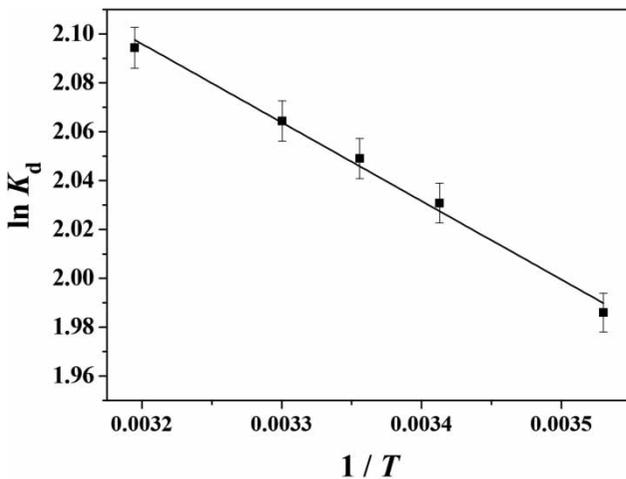

Figure 4 | Reaction thermodynamics of bromate removal on nZVI/MCM-41.

decreased, which explained that at this stage adsorption is dominant. After that, the bromine ions could be detected in the solution, and the concentration increased with the increase of time. The concentration of bromine ions is less

Table 1 | Thermodynamic data for the removal of bromate

T (K)	K_d	ΔG (KJ/moL)	ΔS (J/(moL·K))	ΔH (KJ/moL)
283	7.28	−4.67	25.94	2.67
293	7.62	−4.95		
298	7.76	−5.08		
303	7.88	−5.20		
313	8.12	−5.45		
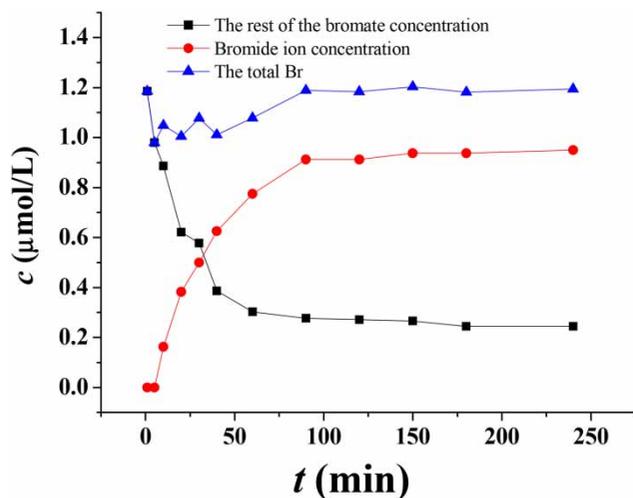
Figure 5 │ Analyzed curves of bromate adsorption and reduction.

Table 2 │ Constants and correlation coefficients of adsorption isotherms for the adsorption

Model	Parameter	Bromate
Temkin equation	b_T	3.61
	A_T	0.47
	R^2	0.951
Dubinin–Radushkevich equation	B (g^2/kJ^2)	7.20
	q_m (mg/g)	5.52
	R^2	0.918
Henry equation	K_h	2.86
	R^2	0.66
Freundlich equation	K_f	5.52
	N	5.61
	R^2	0.918
Langmuir equation	q_m (m/g)	4.98
	K_L	32.45
	R^2	0.998

than that of bromate. It showed that in 30 minutes, adsorption is still the dominant effect. After 30 min, bromine ions continued to rise and bromate decreased, and achieved balance after the 60 min.

From the whole process we could infer that the bromate removal process was one of adsorption and reduction synergies. Firstly, bromate was adsorbed onto the surface of nZVI/MCM-41, and then reduced by nZVI/MCM-41.

Adsorption isotherms

In the first adsorption process (0–30 min), the adsorption capacities of the as-obtained nZVI/MCM-41 for bromate were measured individually at pH 6.5 with 25 mg of nZVI/MCM-41 and varied bromate concentration (0.1–0.8 mg/L). The Henry, Langmuir, Freundlich, and Temkin equations were used for modeling these adsorption isotherm data. The fitted constants along with regression coefficients (R^2) are summarized in Table 2.

Temkin equation:

$$q_e = \frac{RT}{b_T} \ln(A_T c_e) \tag{7}$$

Dubinin–Radushkevich equation:

$$\ln q_e = \ln q_m - \beta \varepsilon^2 \tag{8}$$

Henry equation:

$$q_t = kc \tag{9}$$

Freundlich equation:

$$q_e = K_F c_e^{1/n} \tag{10}$$

Langmuir equation:

$$q_e = \frac{K_L q_{max} c_e}{1 + K_L c_e} \tag{11}$$

The data of the bromate adsorbed at equilibrium (q_e, mg/g) were fitted to the Langmuir adsorption model from Figure 6. Therefore, the adsorptions of bromate onto nZVI/MCM-41 are monolayer uniform adsorptions. The calculated maximum adsorption capacity (q_m) of 4.98 mg/g for bromate is close to the actual measured value of 5.8 mg/g.

CONCLUSIONS

In the study, nZVI/MCM-41 was prepared, and batch equilibrium removal of bromate onto nZVI/MCM-41 was carried out. Removal of the bromate onto nZVI/MCM-41 reaches equilibrium within 60 min at pH 6.5, and agrees well with first-order kinetic models and the Langmuir adsorption model. The product analysis found that in the process of
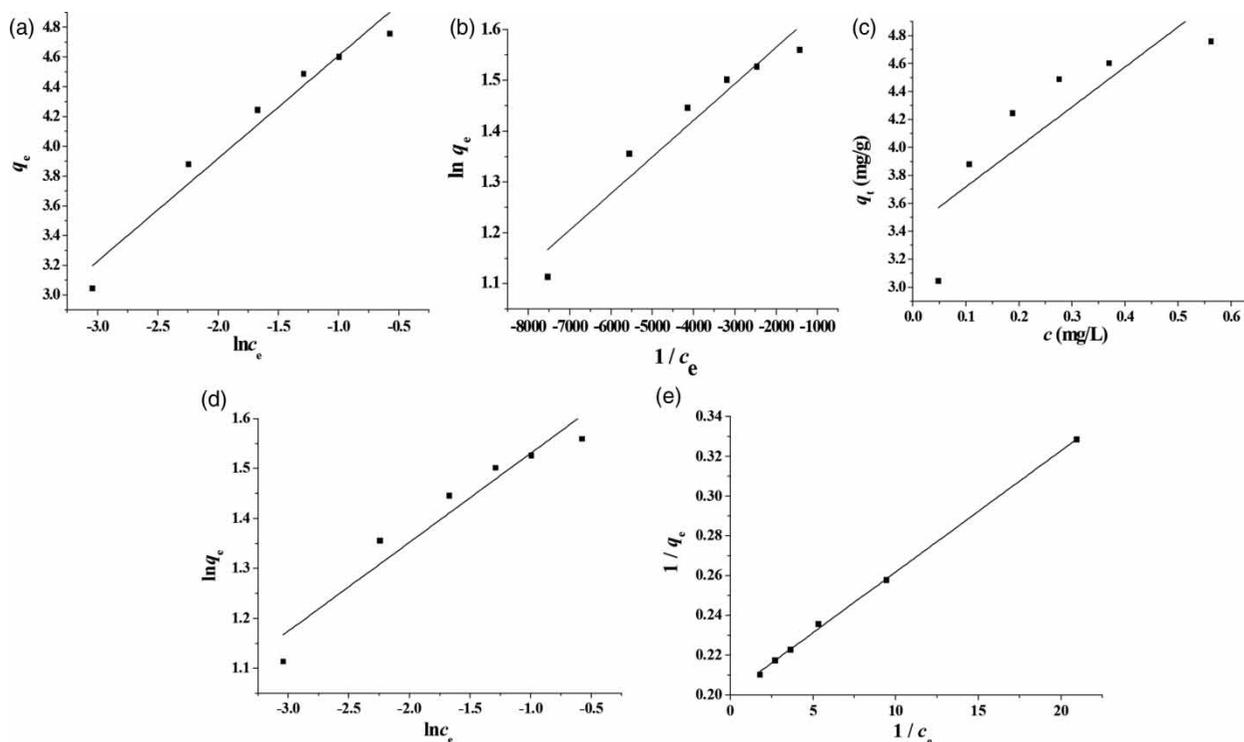
Figure 6 | (a) Temkin, (b) Dubinin–Radushkevich, (c) Henry, (d) Freundlich and (e) Langmuir fit of bromate adsorption on nZIV/MCM-41.

removal, adsorption and reduction exist at the same time, and 30 min was the cut-off point for the amount of removed quantity. Furthermore, the reduction reaction occurred after the adsorption reaction, which showed that the bromate removal process was one of adsorption and reduction synergies.

ACKNOWLEDGEMENTS

REFERENCES

Chitrakar, R., Makita, Y., Sonoda, A. & Hirotsu, T. 2011 Adsorption of trace levels of bromate from aqueous solution by organo-montmorillonite. *Appl. Clay Sci.* **51**, 375–379.

Cho, D. W., Song, H., Schwartz, F. W., Kim, B. & Jeon, B.-H. 2015 The role of magnetite nanoparticles in the reduction of nitrate in groundwater by zero-valent iron. *Chemosphere* **125**, 41–49.

Chun, C. L., Baer, D. R., Matson, D. W., Amonette, J. E. & Penn, R. L. 2010 Characterization and reactivity of iron nanoparticles prepared with added Cu, Pd and Ni. *Environ. Sci. Technol.* **44**, 5079–5085.

Chytil, S., Glomm, W. R., Vollebekk, E., Bergem, H., Walmsley, J., Sjöblom, J. & Blekkan, E. A. 2005 Platinum nanoparticles encapsulated in mesoporous silica: preparation, characterisation and catalytic activity in toluene hydrogenation. *Micropor. Mesopor. Mat.* **86**, 198–206.

Dimos, K., Stathi, P., Karakassides, M. A. & Deligiannakis, Y. 2009 Synthesis and characterization of hybrid MCM-41 materials for heavy metal adsorption. *Micro. Meso. Mater.* **126**, 65–71.

Fan, J., Shui, W. Q., Yang, P. Y., Wang, X. Y., Xu, Y. M., Wang, H. H., Chen, X. & Zhao, D. Y. 2005 Mesoporous silica nanoreactors for highly efficient proteolysis. *Chem-Eur. J.* **11**, 5391–5396.

Ginkel, C. G. v., Haperen, A. M. v. & Togt, B. v. d. 2005 Reduction of bromate to bromide coupled to acetate oxidation by anaerobic mixed microbial cultures. *Water Res.* **39**, 59–64.

Gunten, U. v. 2003 Ozonation of drinking water: part II. Disinfection and by-product formation in presence of bromide, iodide or chlorine. *Water Res.* **37**, 1469–1487.

Hrudey, S. E. 2009 Chlorination disinfection by-products, public health risk tradeoffs and me. *Water Res.* **43**, 2057–2092.

Hwang, B. F. & Jaakkola, J. J. K. 2003 Water chlorination and birth defects: a systematic review and meta-analysis. *Arch. Environ. Health* **58**, 83–91.

Jia, H. Z., Gu, C., Boyd, S. A., Teppen, B. J., Johnston, C. T., Song, C. Y. & Li, H. 2011 Comparison of reactivity of nanoscaled zero-valent iron formed on clay surfaces. *Soil Sci. Soc. Am. J.* **75**, 357–364.

Khalil, A. M. E, Eljamal, O., Amen, T. W. M., Sugihara, Y. & Matsunaga, N. 2017 Optimized nano-scale zero-valent iron supported on treated activated carbon for enhanced nitrate and phosphate removal from water. *Chem. Eng. J.* **309**, 349–365.

Kong, L. B., Li, H., Zhang, J., Luo, Y. C. & Kang, L. 2010 Platinum catalyst on ordered mesoporous carbon with controlled morphology for methanol electrochemical oxidation. *Appl. Surf. Sci.* **256**, 6688–6693.

Krasner, S. W., Glaze, W. H., Weinberg, H. S., Daniel, P. A. & Najm, I. N. 1993 Formation and control of bromate during ozonation of waters containing bromide. *J. Am. Water Works Assoc.* **85**, 73–81.

Krasner, S. W., Weinberg, H. S., Richardson, S. D., Pastor, S. J., Chinn, R., Sclimenti, M. J., Onstad, G. D. & Thruston, A. D. 2006 Occurrence of a new generation of disinfection byproducts. *Environ. Sci. Technol.* **40**, 7175–7185.

Li, Y., Zhang, Y., Li, J. & Zheng, X. 2011 Enhanced removal of pentachlorophenol by a novel composite: nanoscale zero valent iron immobilized on organobentonite. *Environ. Pollut.* **159**, 3744–3749.

Lin, K. Y. A. & Lin, C. H. 2017 Enhanced reductive removal of bromate using acid-washed zero-valent iron in the presence of oxalic acid. *Chem. Eng. J.* **325**, 144–150.

Ling, L., Pan, B. & Zhang, W. 2015 Removal of selenium from water with nanoscale zero-valent iron: mechanisms of intraparticle reduction of Se(IV). *Water Res.* **71**, 274–281.

Liu, H., Li, Y., Wu, H., Yang, W. & He, D. 2014 Promoting effect of glucose and β-cyclodextrin on Ni dispersion of Ni/MCM-41 catalysts for carbon dioxide reforming of methane to syngas. *Fuel* **136**, 19–24.

Liu, Y., Zhang, Y. & Ni, B. 2015 Zero valent iron simultaneously enhances methane production and sulfate reduction in anaerobic granular sludge reactors. *Water Res.* **75**, 292–300.

Lv, X. S., Xu, J., Jiang, G. M. & Xu, X. H. 2011 Removal of chromium(VI) from wastewater by nanoscale zero-valent iron particles supported on multiwalled carbon nanotubes. *Chemosphere* **85**, 1204–1209.

Lyubchik, S. I., Lyubchik, A. I., Galushko, O. L., Tikhonova, L. P., Vital, J., Fonseca, I. M. & Lyubchik, S. B. 2004 Kinetics and thermodynamics of the Cr(III) adsorption on the activated carbon from co-mingled wastes. *Colloids Surf. A* **242**, 151–158.

Meunier, L., Canonica, S. & Gunten, U. v. 2006 Implications of sequential use of UV and ozone for drinking water quality. *Water Res.* **40**, 1864–1876.

Moore, M. M. & Chen, T. 2006 Mutagenicity of bromate: implications for cancer risk assessment. *Toxicology* **221**, 190–196.

Nakatsuji, Y., Salehi, Z. & Kawase, Y. 2015 Mechanisms for removal of p-nitrophenol from aqueous solution using zero-valent iron. *J. Environ. Manage.* **152**, 183–191.

Nieuwenhuijsen, M. J. 2005 Adverse reproductive health effects of exposure to chlorination disinfection by-products. *Global NEST J.* **7**, 128–144.

Pan, H., Wang, J., Chen, L., Su, G., Cui, J., Meng, D. & Wu, X. 2013 Preparation of sulfated alumina supported on mesoporous MCM-41 silica and its application in esterification. *Catal. Commun.* **35**, 27–31.

Petala, E., Dimos, K., Douvalis, A., Bakas, T., Tucek, J., Zbořil, R. & Karakassides, M. A. 2013 Nanoscale zero-valent iron supported on mesoporous silica: characterization and reactivity for Cr(VI) removal from aqueous solution. *J. Hazard. Mater.* **261**, 295–306.

Phenrat, T., Saleh, N., Sirk, K., Tilton, R. D. & Lowry, G. V. 2006 Aggregation and sedimentation of aqueous nanoscale zerovalent iron dispersions. *Environ. Sci. Technol.* **41**, 284–290.

Richardson, S. D. 2005 New disinfection by-product issues: emerging DBPs and alternative routes of exposure. *Global NEST J.* **7**, 43–60.

Segura, Y., Martínez, F., Melero, J. A. & Fierro, J. L. G. 2015 Zero valent iron (ZVI) mediated Fenton degradation of industrial wastewater: treatment performance and characterization of final composites. *Chem. Eng. J.* **269**, 298–305.

Sleiman, N., Deluchat, V., Wazne, M., Mallet, M., Courtin-Nomade, A., Kazpard, V. & Baudu, M. 2017 Phosphate removal from aqueous solutions using zero valent iron (ZVI): influence of solution composition and ZVI aging. *Colloid Surf. A* **514**, 1–10.

Wakayama, H., Setoyama, N. & Fukushima, Y. 2003 Size-controlled synthesis and catalytic performance of Pt nanoparticles in micro- and mesoporous silica prepared using supercritical solvents. *Adv. Mater.* **15**, 742–745.

Wang, W., Zhou, M., Jin, Z. & Li, T. 2010 Reactivity characteristics of poly(methyl methacrylate) coated nanoscale iron particles for trichloroethylene remediation. *J. Hazard. Mater.* **173**, 724–730.

Weinberg, H. S., Delcomyn, C. A. & Unnam, V. 2003 Bromate in chlorinated drinking waters: occurrence and implications for future regulation. *Environ. Sci. Technol.* **37**, 3104–3110.

Wiśniewski, J. A. & Kabsch-Korbutowicz, M. 2010 Bromate removal in the ion-exchange process. *Desalination* **261**, 197–201.

Xie, L. & Shang, C. 2007 The effects of operational parameters and common anions on the reactivity of zero-valent iron in bromate reduction. *Chemosphere* **66**, 1652–1659.

Xu, C., Lin, S., Wang, X., Chen, Y., Zhu, L. & Wang, Z. 2014 Ordered mesoporous carbon immobilized nano zero-valent iron in bromate removal from aqueous solution. *J. Taiwan Inst. Chem. Eng.* **45**, 3000–3006.

Zhang, Y., Li, Y., Li, J., Hu, L. & Zheng, X. 2011 Enhanced removal of nitrate by a novel composite: nanoscale zero valent iron supported on pillared clay. *Chem. Eng. J.* **171**, 526–531.

Zhou, Z., Ruan, W., Huang, H., Shen, C., Yuan, B. & Huang, C. 2016 Fabrication and characterization of Fe/Ni nanoparticles supported by polystyrene resin for trichloroethylene degradation. *Chem. Eng. J.* **283**, 730–739.